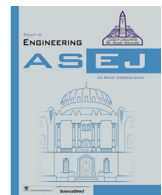




Contents lists available at ScienceDirect

Ain Shams Engineering Journal

journal homepage: www.sciencedirect.com



A robust and efficient EEG-based drowsiness detection system using different machine learning algorithms



Islam A. Fouad

Biomedical Engineering Dept., MUST University, Giza, Egypt

ARTICLE INFO

Article history:

Received 1 January 2022

Revised 11 June 2022

Accepted 13 July 2022

Available online 01 August 2022

Keywords:

Drowsiness detection

Electroencephalography (EEG)

Linear discriminant analysis (LDA)

Support vector machine -RBF (SVM-rbf)

K-Nearest Neighbor (KNN)

Random forest (RF)

ABSTRACT

Vehicle accidents on long routes around the world are frequently caused by drowsy drivers. It is mainly because there is no system that measures alertness. The driver will be notified to interrupt his/her travel if an accurate and robust fatigue detection system is available. Dealing with this approach will help the driver avoid accidents and make the right decisions.

This paper aims to detect drivers' sleepiness using a powerful software tool. It was initially developed by capturing electroencephalography (EEG) signals and processing them.

In this research, different machine learning algorithms were applied to the EEG signals of twelve subjects to measure their performance. In the first step, all recorded data for all subjects were segmented into second epochs. Brain signals were labeled alert or drowsy for each epoch.

Before applying the machine learning algorithms to the epoched signal, a preprocessing step is introduced to extract the relevant features. The applied algorithms are: Naive Bayes (Diagonal Linear Discriminant Analysis), Support Vector Machines (Linear and Radial Basis Functions), K-Nearest Neighbor (KNN), and Random Forest Analysis (RFA). By capturing signals from only three electrodes, it was found that utilizing more than one classifier led to the highest accuracy of 100% for all subjects considered in this study.

In general, this developed EEG-based system detects drowsiness and loss of focus of drivers in real-time with high accuracy, making it a practicable and reliable option for real-time applications.

© 2022 THE AUTHOR. Published by Elsevier BV on behalf of Faculty of Engineering, Ain Shams University. This is an open access article under the CC BY-NC-ND license (<http://creativecommons.org/licenses/by-nc-nd/4.0/>).

1. Introduction

In several countries, driver drowsiness has been identified as one of the leading causes of traffic accidents. Many studies have been conducted over the years to identify drowsiness and warn the driver in order to reduce the number of accidents. Some of the main terms, driver vigilance monitoring, drowsiness detection systems, and fatigue monitoring systems are used to identify the device that detects driver drowsiness in a 2006 study regarding fatigue [1]. Many useful indicators can be used to track and assess driver drowsiness. Indicators that are objective Electro-oculogram (EOG), facial expressions and shifts, yawning, eye movement, heart

rate, breathing rate, skin conductance, and steering wheel grip are all examples of brain signals. Subjective techniques, such as KSS, are used during, before, and after the driving task. Lane lateral deviation and steering wheel movement rates are two other metrics that measure the vehicle's driving efficiency. Drowsiness and alertness were measured and graded in real-world driving, simulated driving tasks in simple setups, and simulated driving in complex setups in specialized laboratories [2–11].

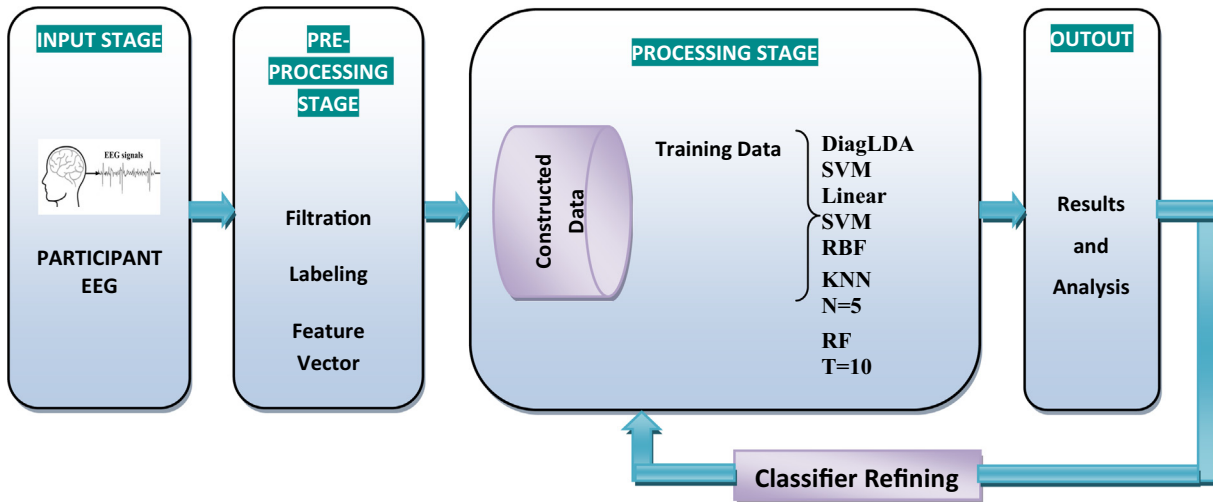
One of the physiologic markers that can track human actions, etiquette, and mental state is brain signals. In recent years, the electroencephalograph (EEG) has been designed to record brain signals without the need for complicated setups, which has stifled the use of brain signals in brain-computer interfaces [12]. EEG recording technology has advanced significantly. Dry electrodes may be used to record acquiring signals. Noise and artifact removal software is also integrated into the systems. There have been several studies on brain signals and drowsiness detection, with the conclusion that EEG signals are one of the strongest measures of drowsiness and alertness variance [13]. The time and spectral domains of EEG signals can be analyzed. Signal processing

E-mail address: islam.fouad@must.edu.com

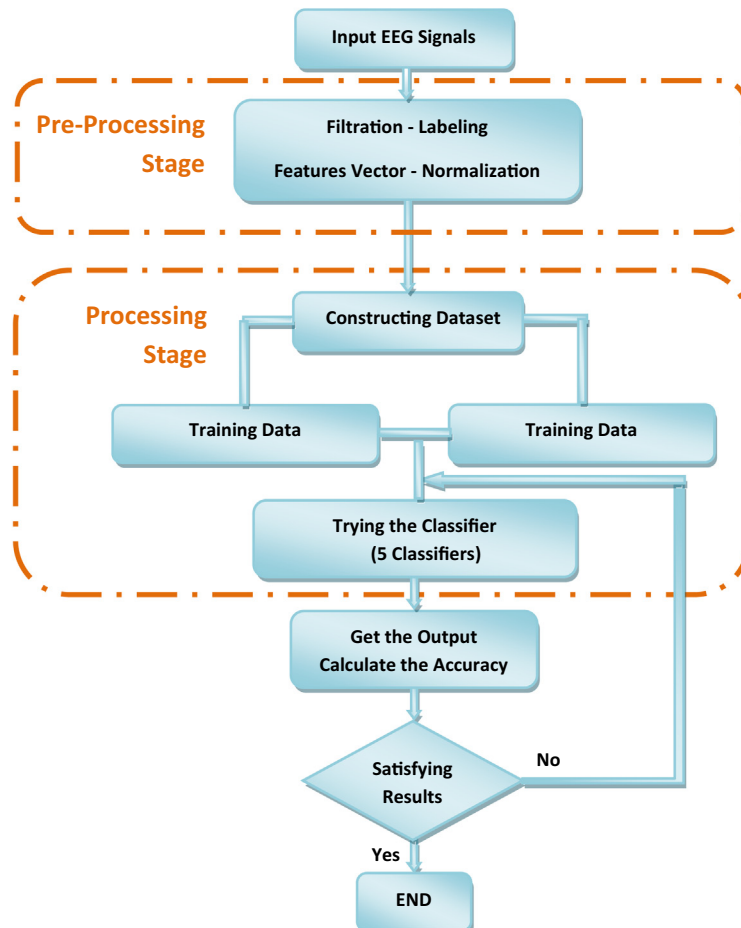
Peer review under responsibility of Ain Shams University.



Production and hosting by Elsevier



(a) Block Diagram of the suggested system.



(b) Flow chart of the suggested system

Fig. 1. Description of the whole proposed system.

techniques, feature extraction methods, and classification methods all play a role in drowsiness detection using EEG. Fast Fourier transformation and discrete wavelet decomposition are two major feature extraction methods that have shown high efficiency in

many studies in this field. In addition, support vector machines have shown excellent classification results [14–23].

The main goal of this study is to develop a drowsiness detection algorithm based on the difference in EEG signals at prefrontal brain

sites Fp1 and Fp2, compared to the reference Fpz, in two vigilance states. These forehead locations were chosen to allow for future realistic implementation of a wireless drowsiness detection device that relies on minimal electrodes and dry electrodes technology to acquire EEG signals. The EEG signals were segmented into five-second epochs and vigilance states were assigned.

Changes in facial expressions and posture were used to categorize the EEG signals as warning or drowsy. Based on facial indicators, observers rated sleepiness and alertness using observer ratings of drowsiness (ORD) criteria. These indicators included rubbing and scratching of face, head, or neck, yawning, restless movement in a chair (e.g., changing posture), drooping head, sluggish eye closures, rolling back of eyes, and squinting eyes. One of the first versions of ORD was created in 1994 [24] and has been analyzed and demonstrated to be effective by several researchers [25–27].

Many researchers used Fp1 alone or in combination with other EEG data from various brain sites. To improve the accuracy percentage of classification between different vigilance states, various feature extraction and classification methods were tested.

Using wavelet packet decomposition and Gaussian KPCA with SVM, the highest classification accuracy was 98.8% [28]. The features were determined for each epoch using an eight-octave wavelet packet decomposition, relative wavelet packet energy for the delta (0.5–3.5 Hz), theta (4–7 Hz), alpha (8–12 Hz), and beta (13–30 Hz) frequency bands, and the ratio indices beta/alpha, theta/alpha, (alpha + theta)/beta for each of the channels (Fp1, Fp2). Another study found using wavelet packet energy (WPE) of EEG to extract features and random forest (RF) to pick key features for differentiating the two states resulted in a 97% accuracy [29].

In two experiments using statistical features in the time domain maximum and minimum values of each signal, mean values, standard deviation, and the median values, and neural network classifier with backpropagation, the average accuracy was 97.3% and

Table 1
Values of Support Vector Machine Hyper-parameters.

Standardize	Kernel Scale	Kernel Function	SVM Method
True	27.1	Linear	Method I
True	2.1	RBF	Method II

98%, respectively [30,31]. EEG signals were reported from sixty subjects who had been awake for twenty-four hours and were doing a real driving activity with a Neurosky mobile mindset (dry electrode at Fp1) [30,31].

Using EEG and respiration signals, the identification accuracy was 98.6% [32]. To select the most descriptive features for further classification, EEGs were preprocessed with a Butterworth band-pass filter, feature extractor wavelet-packet-transform (WPT) system, and mutual information (MI) technique. A support vector machine (SVM) [33] was used to classify the data. The accuracy of Grey Relational Analysis (GRA) to identify the optimal indicator of driver fatigue was 93% for alert and 91.5% for drowsy, after which the number of significant electrodes was reduced using Kernel Principal Component Analysis (KPCA), and the evaluation

Table 2
“Whole Subjects” Accuracies of the Applied Classifiers.

Classifiers	The Whole Subjects 12 Subjects as a unit	
	Cut-off Frequency Range	Accuracy
DiagLDA	0.15–45 Hz	69.77%
SVM Linear		100%
SVM RBF		93.13%
KNN N = 5		100%
RF T = 10		99.88%

Table 3
“Whole Subjects” - Time Taken of the Applied Classifiers.

Classifiers	Whole Subjects	
	Train Time (sec.) / Trial	Test Time (sec.) / Trial
DiagLDA	0.783565	1.670506
SVM Linear	0.669599	1.147101
SVM RBF	0.825558	1.550250
KNN N = 5	0.983565	1.081267
RF T = 10	1.785005	2.293617

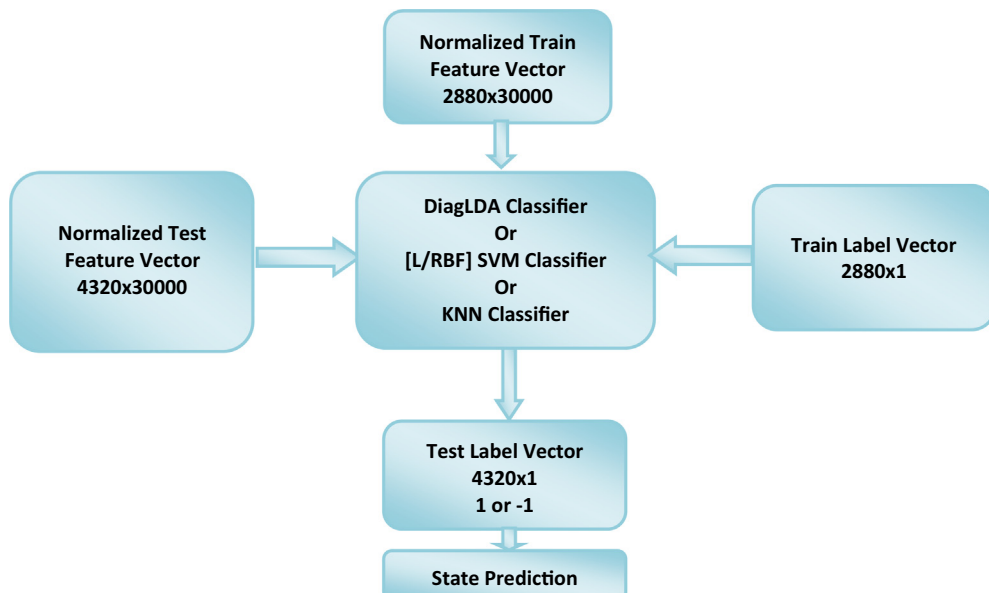


Fig. 2. DiagLDA, SVM, and KNN Classifiers.

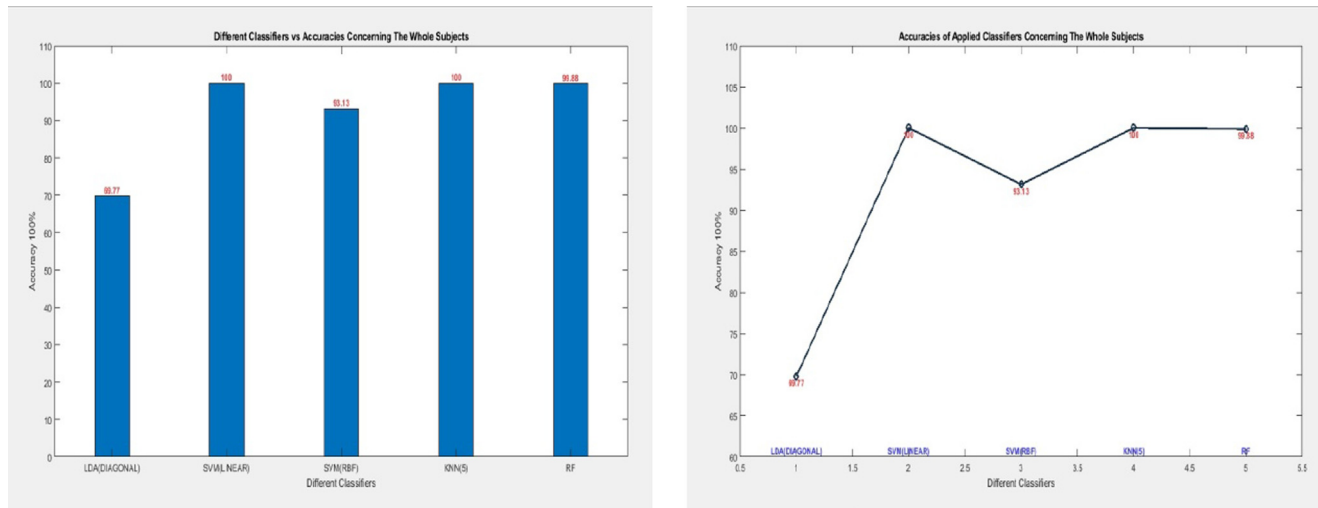


Fig. 3. Accuracies of the Applied Classifiers.

Table 4

"Subjects 1-6" Accuracies of the Applied Classifiers.

Classifiers	Accuracy					
	Subject 1	Subject 2	Subject 3	Subject 4	Subject 5	Subject 6
DiagLDA	100%	100%	100%	100%	100%	100%
LSVM	100%	100%	100%	100%	100%	100%
SVM RBF	49.1667%	57.5%	47.7778%	98.6111%	98.3333%	47.7778%
KNN N = 5	100%	100%	100%	100%	100%	100%
RF T = 10	100%	100%	100%	100%	100%	100%

Table 5

"Subjects 7-12" Accuracies of the Applied Classifiers.

Classifiers	Accuracy					
	Subject 7	Subject 8	Subject 9	Subject 10	Subject 11	Subject 12
DiagLDA	100%	100%	100%	100%	100%	100%
LSVM	100%	100%	100%	100%	100%	100%
SVM RBF	46.6664%	51.1111%	47.5%	49.4444%	48.3333%	50.2778%
KNNN = 5	100%	100%	100%	100%	100%	100%
RFT = 10	100%	100%	100%	100%	100%	100%

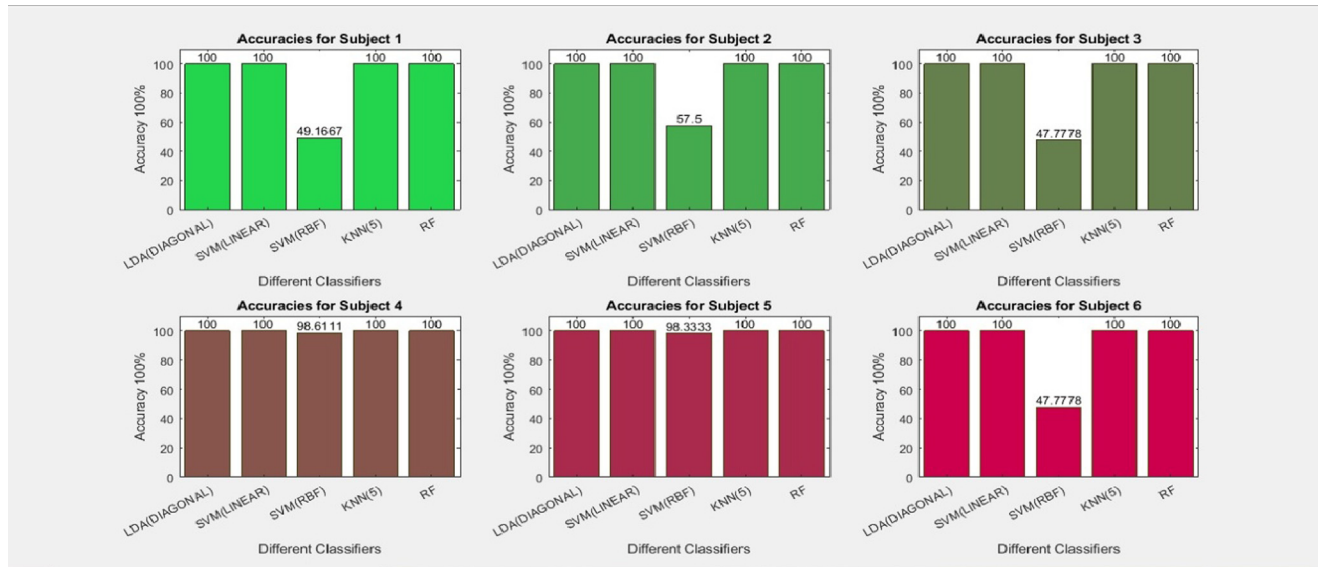


Fig. 4. Accuracies of the Applied Classifiers on Subjects 1-6.

model for driver fatigue was developed with the regression equation based on EEG data from two significant electrodes. With thirty-two channels and an extraction system of autoregressive (AR) model-based power spectral density (PSD) and a classification method of fuzzy particle swarm optimization with a cross mutated artificial neural network (FPSOCMANN), the classification accuracy was 80.51% [34].

Using the stationary wavelet transform to derive two features of the EEG signal and a backpropagation neural network, the accuracy was 79.1% for alertness and 90.91% for drowsiness states [35]. Based on the power spectral density feature extracted by "db4" wavelet function and using a subtractive fuzzy inference classifier [36], the accuracy was 84.41%. Another study found that using wireless EEG signals and a power spectral density function extracted by db4 wavelet and a probabilistic neural network classifier (PNN), the accuracy was 61.16% [37]. Using a hybrid deep generic model (DGM)-based support vector machine, the classifi-

cation accuracy averaged 73.29% [38]. The accuracy for drowsy obtained at electrode P3 was 93.67%, and the specificity for the warning was 88.89% [39]. By using approximate Entropy (AE) and Sample Entropy (SE) to characterize the irregularity and complexity of EEG data and using a Support Vector Machine (SVM) as a classifier, the highest specificity of 91.11% was achieved at electrode P4 [39]. The averaged accuracy in that study was maximum at the P3 electrode, where substantial variations between the two states were 0.022 for AE and 0.026 for SE [39].

Using two tailed t-tests on extracted chaotic features (including Higuchi's fractal dimension and Petrosian's fractal dimension) and the logarithm of signal energy, the accuracy was 83.3% [40]. These features can create a 95% significance level of difference between drowsiness and alertness.

The accuracy was 72% using linear regression and 62% using fuzzy detection [41]. The ocular artifact function was derived using Canonical Correlation Analysis (BSS-CCA) and the wavelet trans-

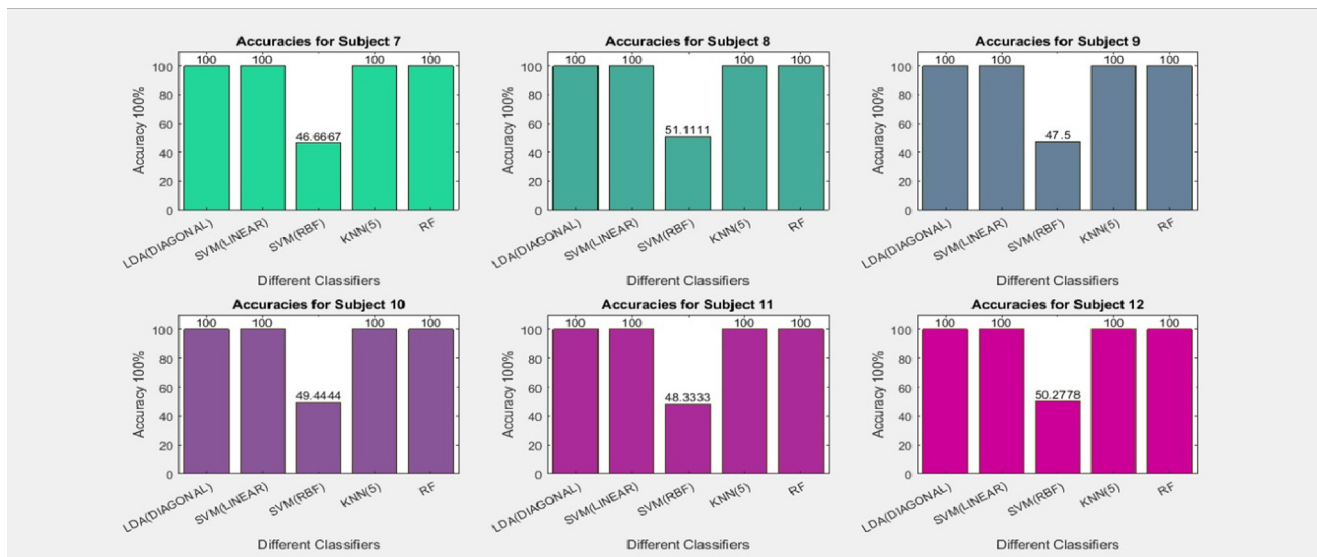


Fig. 5. Accuracies of the Applied Classifiers on Subjects 7–12.

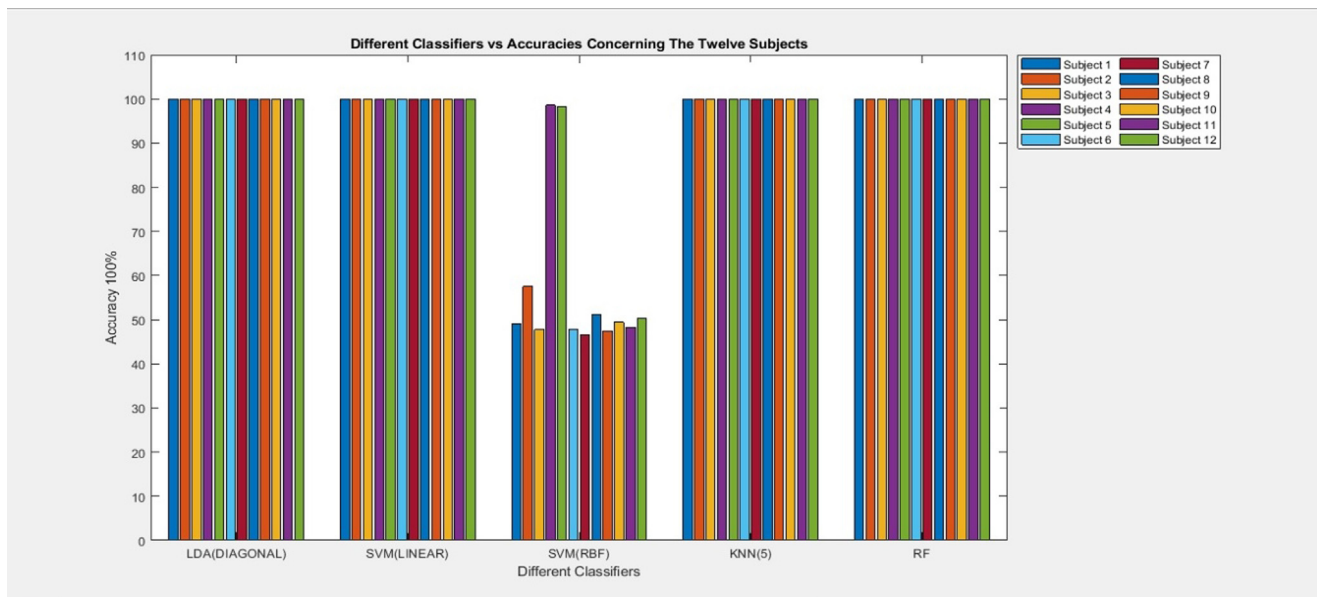


Fig. 6. Accuracies of the Applied Classifiers on All Subjects Individually.

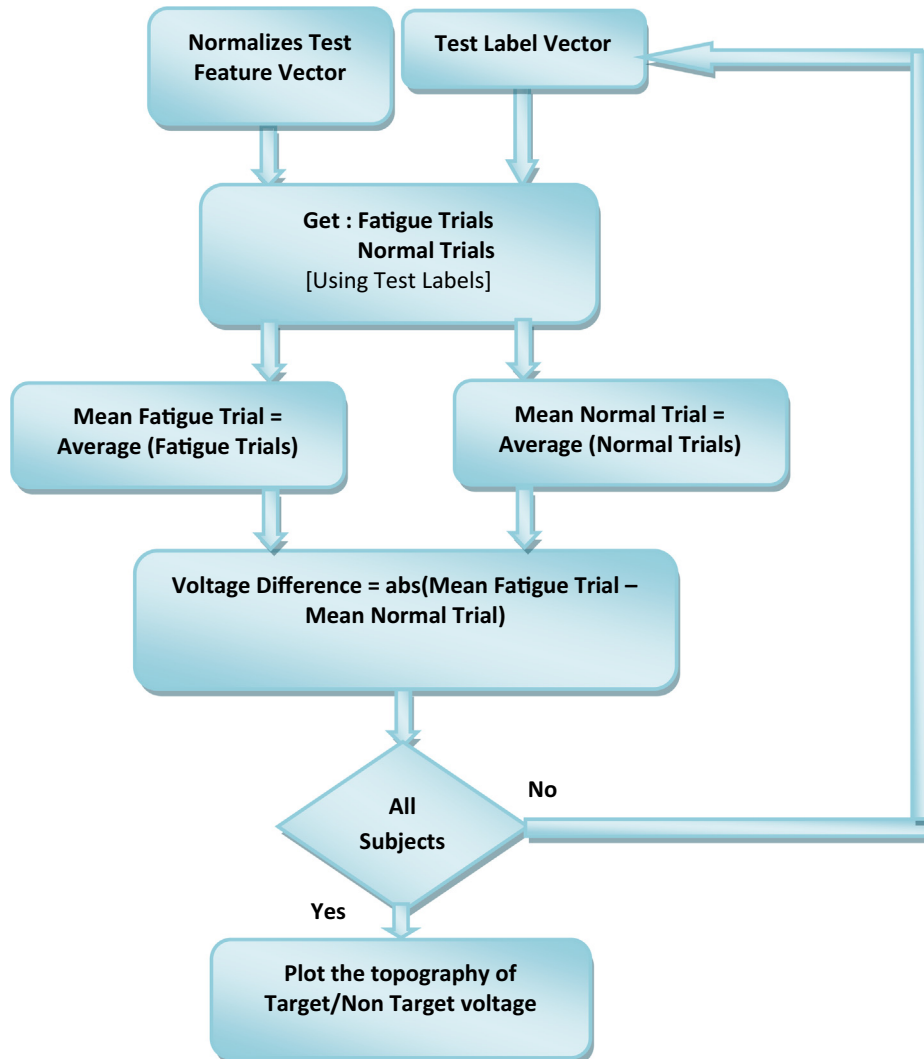


Fig. 7. Flowchart showing procedure used to plot the topography of electrodes for 12 subjects.

form was used to select components containing eye blinks. In a study using three ratio indices and two burst indices calculated from preprocessed EEG signals, β and $(\alpha + \theta)/\beta$ were linked to the mental alertness level [42]. For all four frequency bands, results showed that frontal and occipital inter-hemispheric coherence values were significantly higher than middle, parietal, and temporal sites [43]. The application of the qualified observer rating (TOR) system is best correlated with a combination of ocular parameters, accompanied by EEG alpha bursts indicators and EEG spectrum data [44]. Good performance using a Deep Belief Network (DBN) classifier and fused nonlinear features from specified sub-bands and dynamic analysis [45]. In the wavelet domain, the patterns of entropies during different stages of fatigue were evaluated and validated using standard subjective measures [46].

Balam et al. [47] used a convolutional neural network (CNN) for the classification based on the raw EEG signal from the Cz-Oz channel. They used data from the Sleep-EDF Expanded Database and their ground truth for drowsiness was the S1 sleep stage. Since the authors used a publicly available database, they compared their deep learning (DL) approach with the other feature-based approaches, this gives an accuracy of about 94%. Chaabene et al.

[48] used frequency-domain features for defining the ground truth. They used CNN with raw EEG signal from seven electrodes as input and achieved 90% drowsiness detection accuracy.

Yingying et al. [49] used a Long Short-Term Memory (LSTM) network to classify sleepiness in two classes and their final classification accuracy achieved was 98%. Their ground truth labels for classification were based on the alpha-blocking phenomenon and the alpha wave attenuation-disappearance phenomenon. The authors claimed that these two phenomena represent two different sleepiness levels, relaxed wakefulness, and sleep onset, respectively. The authors used only the O2 channel of the EEG signal and performed a continuous wavelet transform to obtain the PSD. Zou et al. [50] used multiscale PE, multiscale SampEn, and multiscale FuzzyEn. Their ground truth labels were based on Li's subjective fatigue scale and the accuracy achieved was 88.74%.

The goal of the suggested work is the ability to differentiate between mental states, in this case, drowsiness and alertness, using a cap of 32-channel electrodes (thirty essential and two reference channels) depending on the 10-20 system. Data from the sensors are collected, processed, and fed to a machine learning

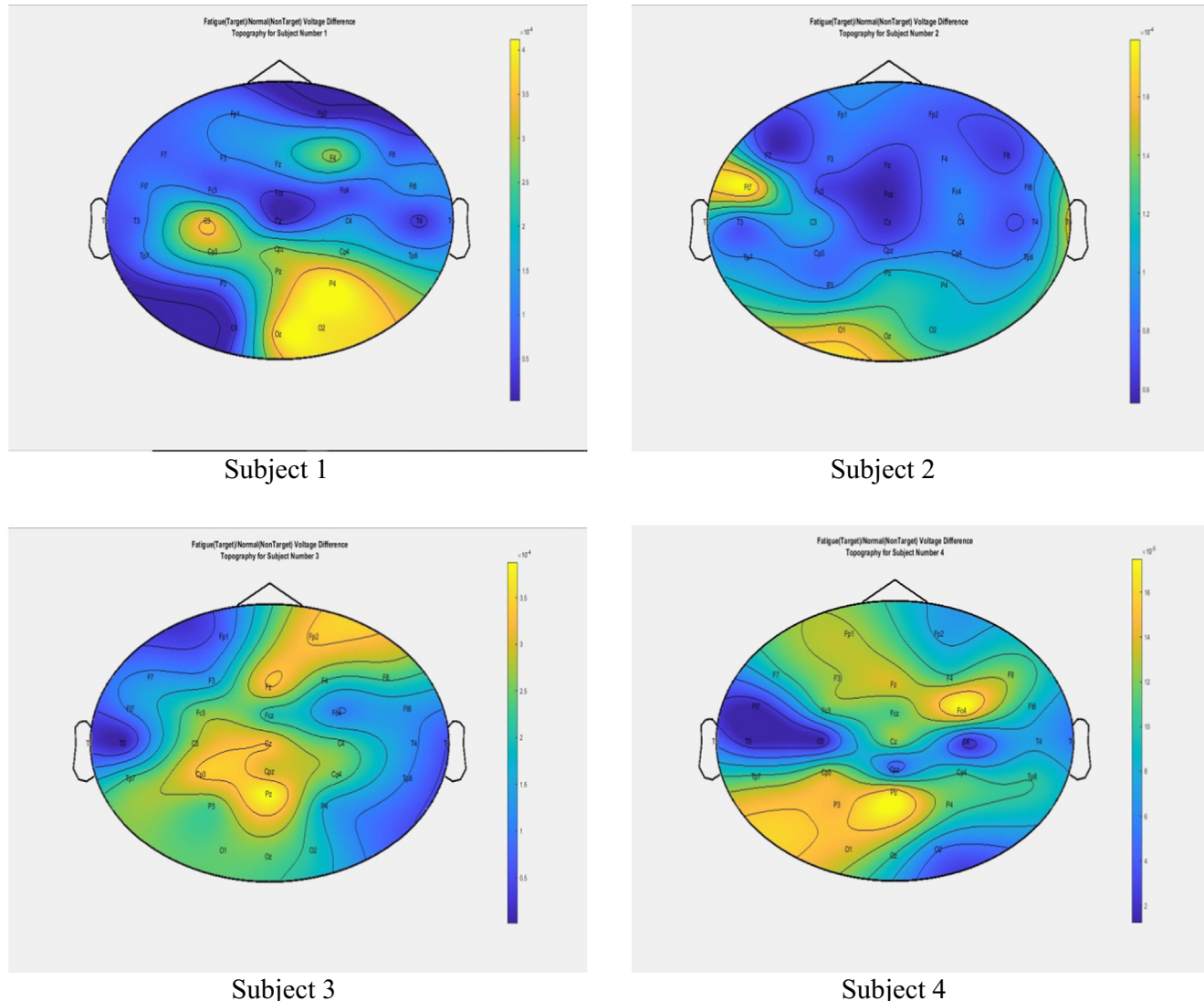


Fig. 8. The channel effectiveness topographies of the twelve subjects. [The effectiveness increased in the locations marked with yellowish color].

algorithm, for data classification. The results using the thirty electrodes and when utilizing only three electrodes are compared, and they show reliability and robustness.

2. Materials

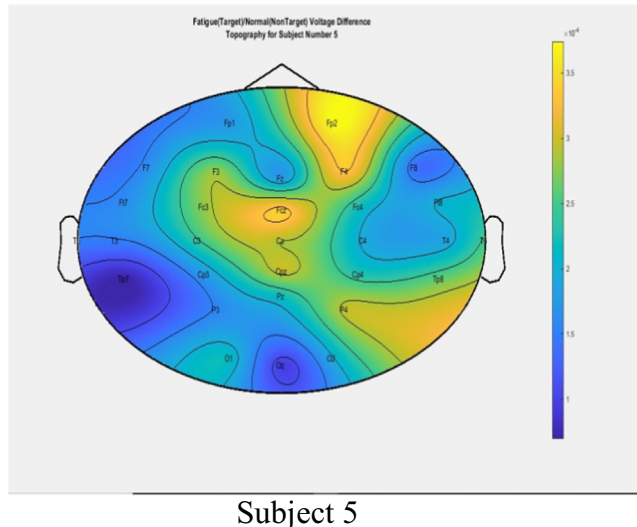
The data that support the findings of this study are openly available at [https://figshare.com/articles/dataset/The_original_EEG_data_for_driver_fatigue_detection/5202739] which was provided by Jianliang Min et al [51]. The data was acquired using a static driving simulator in a controlled lab environment at Jiangxi University of Technology-China. [52].

In this work, MATLAB version 9.9.0.1570001 (R2020b) associated with the Signal Processing Toolbox that helps with a large scale of signal processing functions was utilized for technical computing and data investigation, as it is a high execution and robust tool. This work was implemented using a laptop with a processor type: Intel (R) Core (TM) i7 – 2.7 GHz.

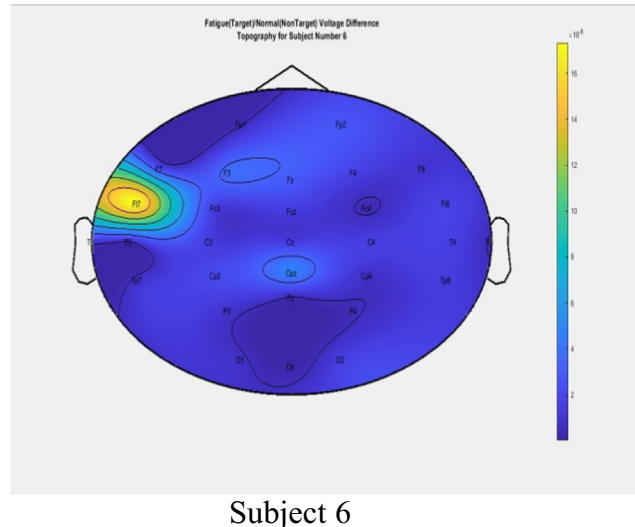
2.1. Data specifications

The obtained signals have the following features:

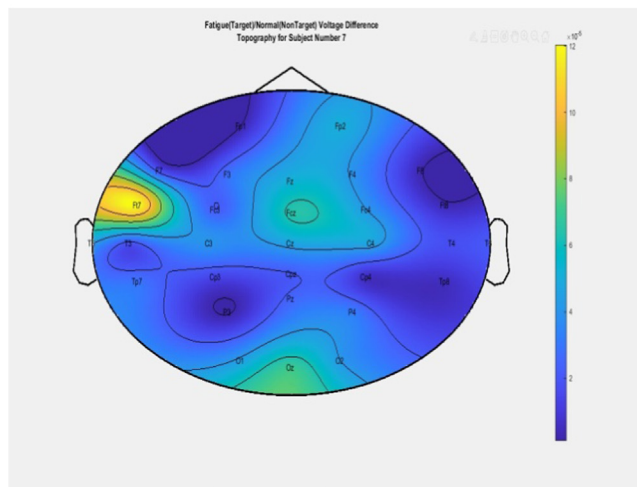
- 12 healthy, young men, with ages from 19 to 24 years, are driving in a highway simulator trial.
- The drivers were burly persons and had an ordinary sleep time.
- The channels data were referred to 2 electrically united mastoids at A1 and A2, sampled at 1000 Hz using a cap of 32-channel electrodes (thirty essential and two reference channels) depending on the 10-20 system.
- The driving duration time was 20 min, then the last 5 min of EEG signals were saved and listed as a normal state.
- The self-reported fatigue questionnaire indicates that the subject was in a driving fatigue state (which will happen after continuous driving for 40 to 100 min), then the last 5 min of EEG signals were saved and listed as a fatigued state.
- The training set consists of 40% of all subjects' EEG for both states: normal and fatigued.



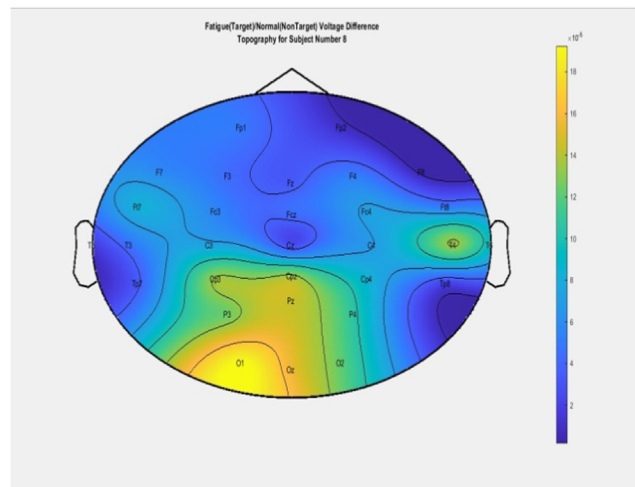
Subject 5



Subject 6



Subject 7



Subject 8

Fig. 8 (continued)

- The testing set consists of 60% of all subjects' EEG for both states: normal and fatigue.
- Data details were well expressed in [51] and [52].

3. Methods

Block diagram and flowchart of the suggested system are shown in Fig. 1.

3.1. Preprocessing

Preprocessing was utilized to minimize the noise and improve the EEG data. It was known that the acquired signals were filtrated with a bandpass filter between 0.15 and 45 Hz and sampled at 1000 Hz.

3.1.1. Trials and filtration

As discussed before there are 12 subjects, and the EEG data for each subject consists of (1000 points [one second] X 30 channels])

as one signal trial. The target is to extract each EEG segment from the given test set to be in the "Normal" or "Fatigue" state.

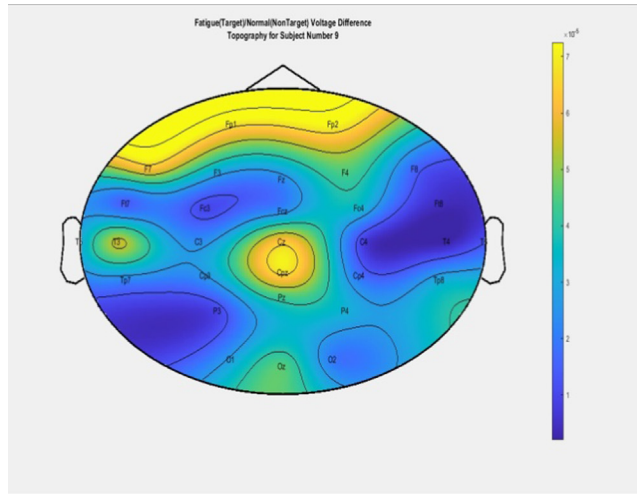
Filtering is a crucial step in minimizing noise. More filtration was applied using an 8th order bandpass filter to the train (240X12 subjects) and test (360X12) segments at cutoff frequencies range (0.15–45 Hz), which was chosen, as the alertness/drowsiness very rarely happened outside that range.

3.2. Feature vector

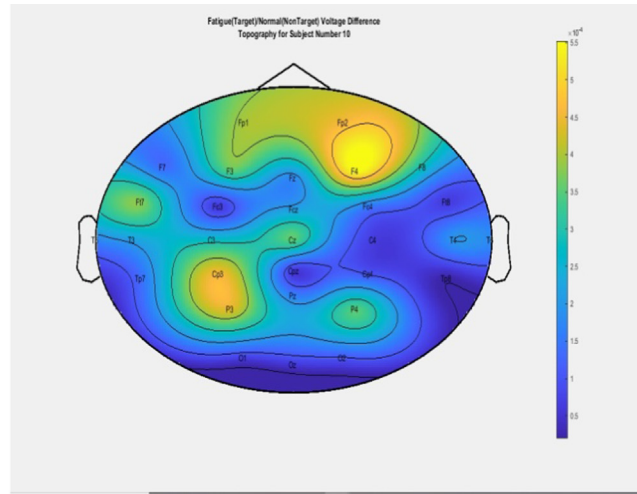
This step is constructed from the succession of the calculations of the 30 channels of all five-minutes (5X60 seconds) segments.

- Total number of segments: $5(\text{min}) * 60(\text{sec}) * 2(\text{Alert and Fatigue states}) = 600 \text{ segments (second epochs)}$

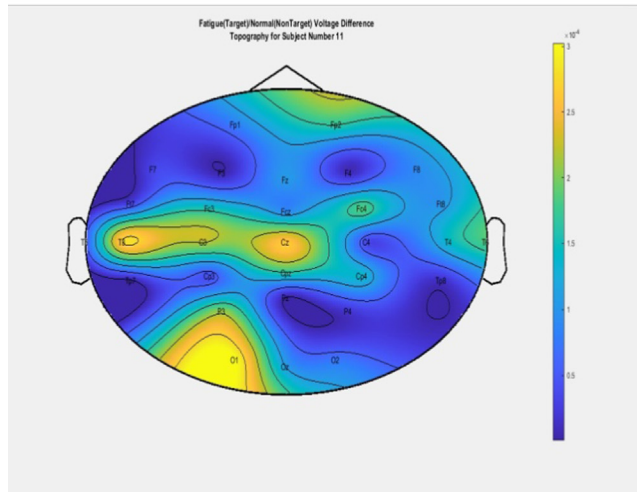
As previously mentioned, the train set of the subject consists of 240 segments (40% of 600); a total of 240X12 (2880) EEG seg-



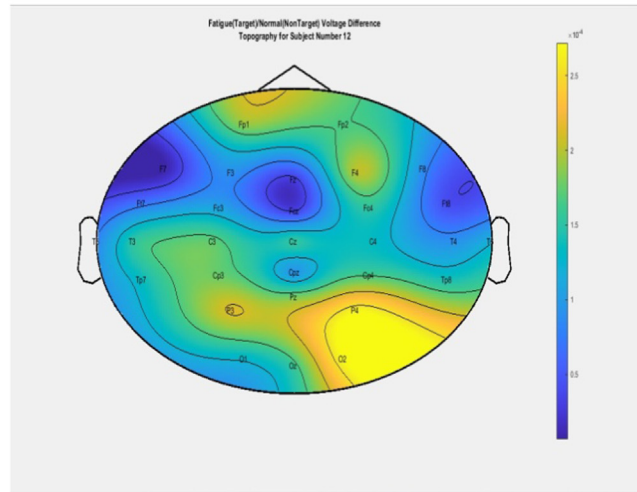
Subject 9



Subject 10



Subject 11



Subject 12

Fig. 8 (continued)

ments, however, the test set of the subject consists of 360 segments; 360X12 (4320) EEG segments.

3.3. Normalization

In machine learning, “Z-Score Normalization” is typically used to handle data that include multiple dimensions. Standardizing the features in the data produces zero-mean (after subtracting the mean in the numerator) and unit variance. To calculate each feature’s mean and standard deviation, we use the distribution mean and standard deviation. This is then subtracted from the respective feature. In the next step, we divide each feature’s values (the mean has already been subtracted) by its standard deviation.

$$x' = \frac{x - \bar{x}}{\sigma}; \text{ } x' \text{ is the normalized feature vector}$$

Where x is the original feature vector (the previously constructed segment), \bar{x} - average (x) is the mean of that feature vector, and σ is its standard deviation.

In the training feature vector, the mean is set to zero, and the variance is set to one. Normalized test feature vectors are then generated using the parameters obtained from normalizing training feature vectors.

3.4. Classification

3.4.1. Diagonal discriminant analysis (Naive Bayes)

Linear classifiers are discriminant algorithms that distinguish various groups using linear functions. They are most definitely the most well-known BCI algorithms.

The aim of LDA is to separate data representing different classes using hyper-planes [53,54]. The class of a function vector in a two-class problem is determined by its position according to the hyper-plane.

Diagonal linear discriminant analysis supposes that the data has a normal distribution and that the diagonal covariance matrices for both groups are equal. The separating hyperplane is found by look-

Table 6

“ Electrodes” Accuracies of the Applied Classifiers.

Electrode	Accuracy %				
	DiagLDA	SVM Linear	SVM RBF	KNN N = 5	RF T = 10
FP1	56.78240741	56.80555556	86.78240741	87.4537037	88.21759259
FP2	61.59722222	65.92592593	86.25	88.84259259	89.05092593
F7	48.44907407	55.48611111	91.43518519	92.66203704	92.89351852
F3	64.81481481	65.76388889	93.0787037	93.05555556	92.73148148
FZ	61.55092593	59.21296296	91.04166667	92.93981481	92.52314815
F4	70.39351852	69.69907407	94.02777778	94.56018519	93.95833333
F8	57.17592593	54.18981481	92.96296296	92.91666667	92.93981481
FT7	51.875	53.51851852	88.10185185	92.82407407	93.61111111
FC3	61.89814815	59.81481481	93.7037037	94.25925926	94.12037037
FCZ	52.87037037	61.50462963	94.14351852	95.94907407	96.13425926
FC4	65.94907407	61.01851852	87.68518519	90.09259259	90.43981481
FT8	54.09722222	61.34259259	91.73611111	91.08796296	91.38888889
T3	51.68981481	49.74537037	89.65277778	90.99537037	91.06481481
C3	52.93981481	56.06481481	94.56018519	93.95833333	94.25925926
CZ	61.59722222	58.1712963	91.94444444	92.52314815	93.00925926
C4	58.88888889	60.71759259	91.45833333	92.4537037	91.64351852
T4	62.06018519	62.89351852	86.96759259	88.47222222	88.61111111
TP7	61.59722222	57.29166667	93.33333333	94.51388889	94.14351852
CP3	61.55092593	57.47685185	94.9537037	95.20833333	94.35185185
CPZ	53.65740741	62.03703704	96.73611111	97.10648148	97.08333333
CP4	57.5462963	57.19907407	92.93981481	92.22222222	92.22222222
TP8	63.93518519	58.14814815	91.34259259	93.05555556	92.43055556
T5	49.12037037	47.63888889	90.87962963	91.38888889	91.41203704
P3	61.85185185	61.85185185	89.97685185	90.87962963	90.74074074
PZ	63.88888889	63.19444444	87.70833333	89.86111111	89.49074074
P4	52.29166667	65.74074074	95.60185185	96.43518519	96.18055556
T6	53.19444444	53.1712963	96.71296296	96.875	96.8287037
O1	57.4537037	55.43981481	94.46759259	92.98611111	93.7037037
OZ	66.80555556	60.5787037	91.27314815	93.65740741	92.40740741
O2	64.51388889	65.97222222	94.28240741	95.97222222	95.13888889

ing for the projection that maximizes the distance between the two class means thus reducing interclass variance [54].

Because of its low computational requirements, this technique is well suited for BCI systems. Furthermore, it is easy to be utilized and produces high performance.

3.4.2. DiagLDA

In the first approach “DiagLDA method”, a test label of ‘1’ was specified as target (Fatigue) or ‘-1’ as non-target (Normal) through each trial.

3.4.3. Support vector machine (SVM)

This classifier is used to classify a group of binary labeled information, this method also utilizes a hyper-plane to divide the data into two groups [55,56]. Then, after training the classifier on a particular dataset, the separately hyper-plane is optimized and chosen depending on the maximum gap between the hyper-plane and that data. This is achieved by changing the data from the input area to the feature area, where linear classification is realized.

A linear support vector machine allows classification using linear decision boundaries. These classifiers have been used to solve large many concurrent BCI problems with great success [57,58,59,60]. It is recommended that kernel functions such as RBF be used whenever the data set is linearly inseparable. The linear kernel function can be used with a linear dataset (kernel=“line ar”). SVM training will be more effective if you know when to use kernel functions.

SVMs have a number of benefits. SVMs are considered to have strong generalization properties [56,61], to be insensitive to overtraining [61], and to be resistant to the curse of dimensionality [55,56].

SVMs have been utilized in brain research because they are a robust pattern recognition approach, particularly used for high-dimensional problems [60].

Two procedures are introduced concerning SVM: “Linear Function” and “Radial Basis Function”.

The chosen value of the regularization parameters (hyper-parameters) via cross-validation of a subset of the train data as a validation set in the previously listed methods is shown in Table 1.

3.4.4. K-Nearest Neighbors (KNN)

K-nearest neighbor (k-n n) is a supervised classification learning method that is used to classify samples. This algorithm’s goal is to identify a new sample using its features and previously labeled training samples [62]. The algorithm is memory-based and does not necessitate the fitting of a model. Given a query point x_0 , the closest k training points (Euclidean distance) to x_0 are found. The new query is assigned to its cluster based on the plurality of its neighbors. Any voting bonds will be broken at random [63].

In the present work, KNN (with $N = 5$) method is performed as a classifier.

Fig. 2 summarizes the previously suggested algorithms.

3.4.5. Random forest classifier

• Explanation

Random forests are machine learning schemes derived from decision trees, where a decision tree is a diagram in the form of a tree that is used to decide a course of action. Each branch of the tree represents a potential choice, event, or reaction [64].

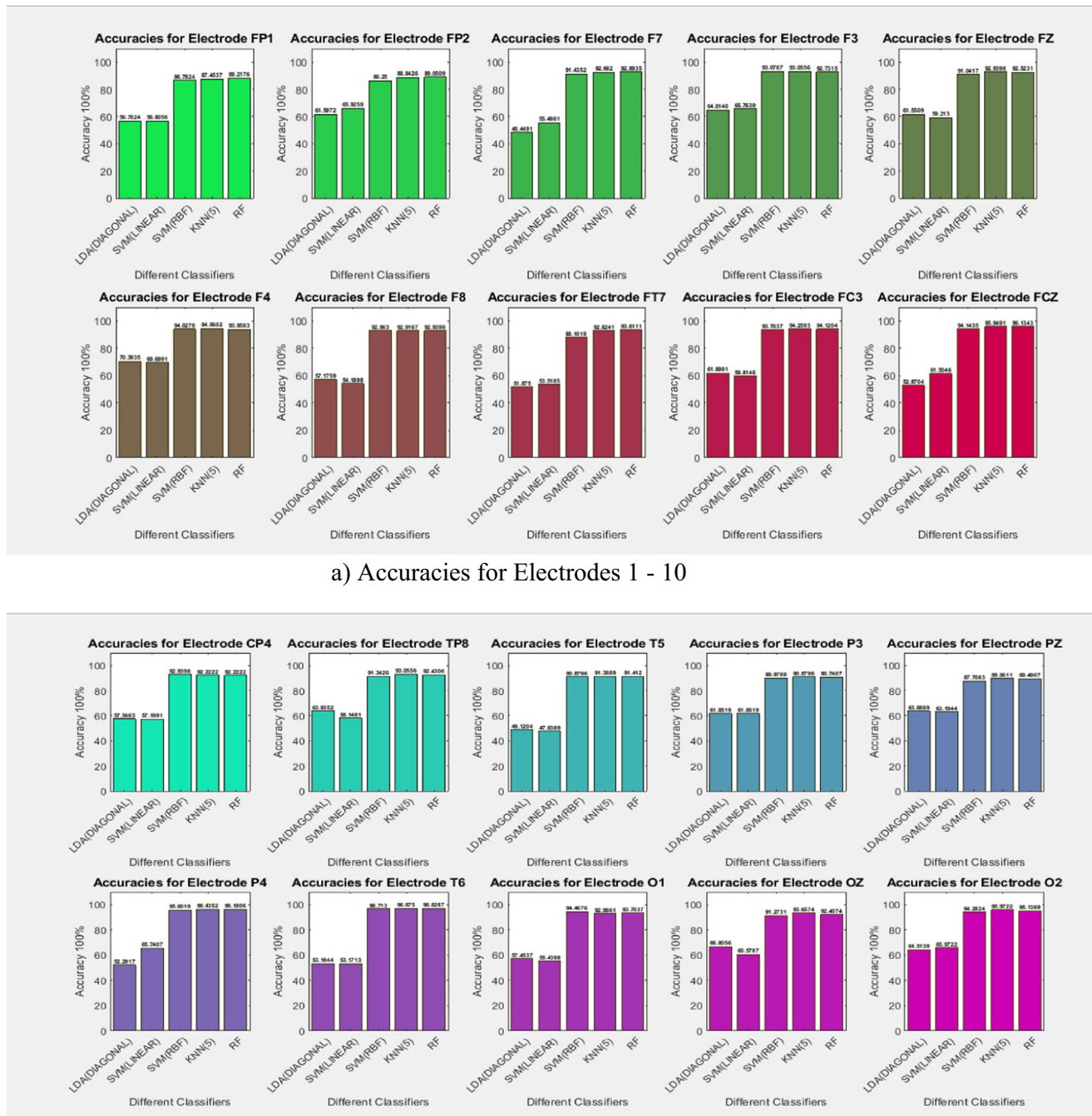


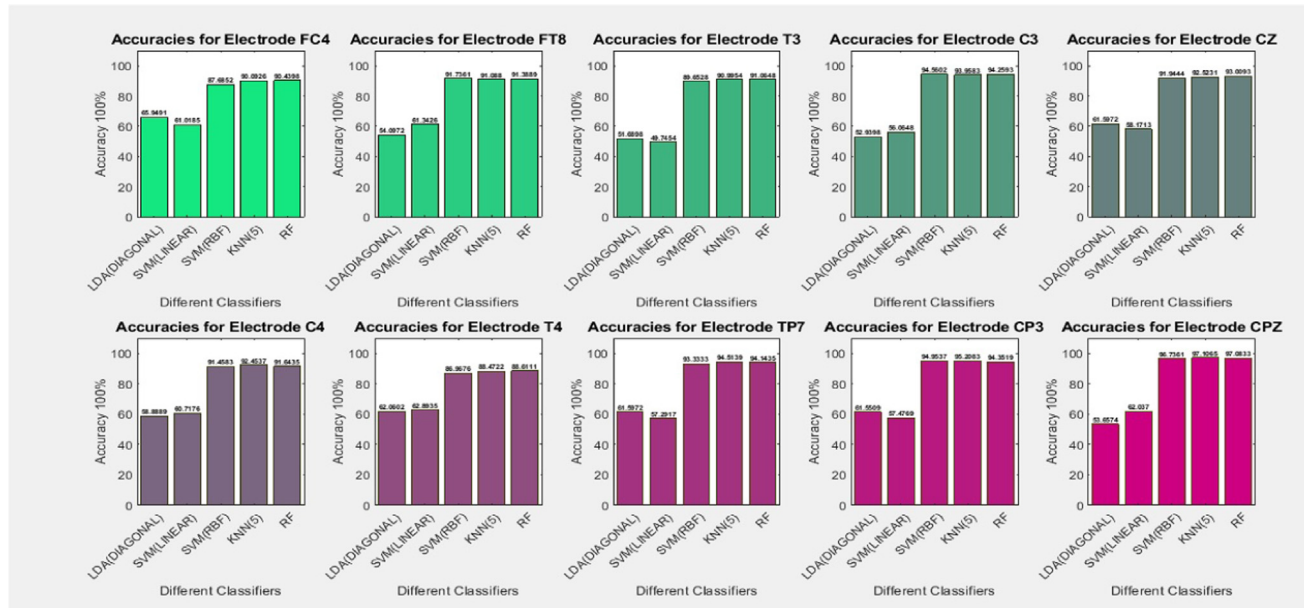
Fig. 9. The accuracies of thirty electrodes.

• Why Random Forests?

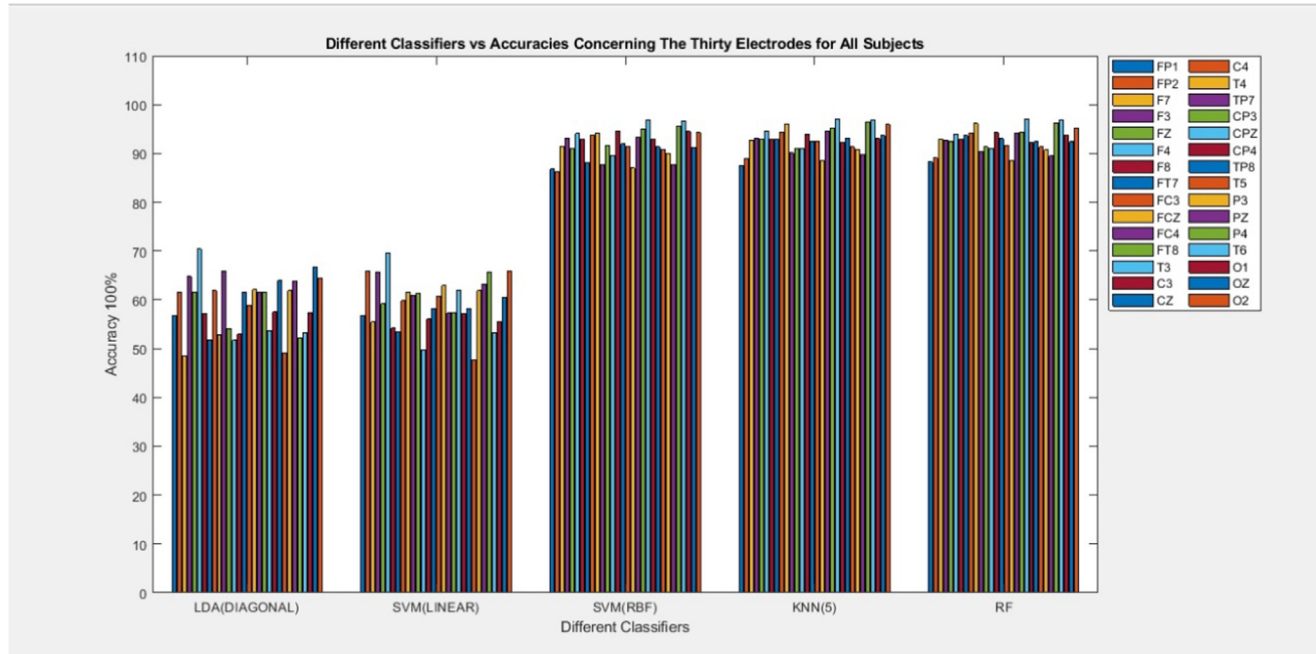
The following are some of the benefits of using Random Forests:

- No over-fitting: using multiple trees decreases the chance of overfitting as well as the amount of time it takes to practice.

- High accuracy: it performs well in large databases and makes highly accurate predictions for large datasets. In today's world of big data, this is critical, and this is likely where Random Forest shines.
- Estimate missing data: When a large percentage of data is missing, Random Forest guesses which one suits best for the missing parameter.



(c) Accuracies for Electrodes 21 - 30



(d) Bar graph of thirty electrodes accuracies

Fig. 9 (continued)

In the present work, a Random Forest classifier (with Number of trees = 10) algorithm is implemented.

• State Prediction

The state is nearly specified from the previously discussed classifiers. The analysis of the work from different aspects will be presented in the following section.

4. Results and discussion

4.1. First: Looking at the twelve subjects simultaneously

Based on the percentage of the correctly estimated trials in the test sets the accuracies are calculated as:

$$\text{Accuracy} = \frac{\text{Correctly estimated trials}}{\text{Total number of trials}} * 100\%$$

Depending on the evaluation standards, **Table 2** shows the accuracies among all subjects and the results for each classifier. The time taken to predict a trial state does not exceed 5 s as shown in **Table 3**. The resulted times are reliable and suitable for online applications.

Fig. 3 shows the accuracies obtained when presenting the discussed classifiers for EEG data taken from all twelve subjects together.

By comparing the accuracies of the proposed classifiers, it is clearly shown that linear support vector machine and KNN algorithms give the highest accuracies, as they performed 100%. However, the DiagLDA method gave the lowest results as it achieved an accuracy of 69.77%. The time taken to apply the given classifiers ranges from 1.081267 to 2.293617 Seconds/ Trial.

4.2. Second: Looking at the twelve subjects individually

Now every subject is taken separately, and the building of training and testing data is based on the same criteria (40% as Training and the remaining 60% as Testing). Based on the percentage of the correctly estimated trials in the test sets, the accuracies are calculated. Depending on the evaluation standards, **Tables 4 and 5** show the accuracies among all subjects and the results for each classifier.

Figs. 4, 5, and 6 show the accuracies obtained when applying the proposed classifiers for EEG data taken from each subject individually.

By comparing the accuracies of the proposed classifiers, it is clearly shown that all classifiers except SVM (RBF) allow the highest performance, as they accomplished 100%. However, SVM (RBF) method gave the lowest results for all subjects except subjects 4 and 5 as it achieved maximum accuracy of 57.5% for the remaining 10 subjects. In general, applying a support vector machine classifier with a 'linear' kernel function gives better results than applying it with 'rbf' kernel function. This is due to the high dimensionality (high number of features) of the EEG signals [65] and it was presented in different EEG applications [66,67].

Now, let's have a look at the responses of the thirty channels and the most effective electrodes for the twelve subjects. **Fig. 7** represents the algorithm for finding the electrode effectiveness in each subject.

Fig. 8 shows the topographies where the subject's priority channels are located in relation to the effectiveness in the cortex. The color denotes a channel's significance in the classification.

By examining the weight-based channel topography of twelve subjects, it can be determined which part of the cortex each subject's priority channels are located. In the suggested classification, the color represents the importance of a channel, and the importance of a channel is based on the weight value it is assigned for each subject.

The chosen electrodes were primarily positioned over specific sections of the cortex region for each participant (subject), as shown in **Fig. 8**. Subjects number 1, 2, 4, 8, 11 and 12 show major variations in the left and middle posterior regions, and the deep color of Subjects number 3, 5, 9, and 10 is visible in the right central region. The allocation of a few important electrodes isn't overly dispersed.

4.3. Third: Looking at each electrode individually

Back to dealing with all twelve subjects simultaneously, again the building of training and testing data as 40% for Training and the remaining for Testing. Based on the percentage of the correctly estimated trials in the test sets, the accuracies are calculated. Depending on the evaluation standards, **Table 6** shows the accuracies among all subjects together and the results for each electrode.

Inspecting the above table yielding that the maximum accuracy is 97.11% obtained from applying KNN classifier on the signal from CPZ electrode, while the minimum accuracy of 47.64% appeared when applying SVM classifier on the signal acquired from T5 channel.

Figs. 9, and 10 show the accuracies obtained from each electrode when applying the proposed classifiers for EEG data taken from all subjects together.

By inspecting the accuracy results of the thirty electrodes using the mentioned classifiers, it is clear from **Figs. 9 and 10** that electrodes number 6[F4], 20[CPZ], and 30[O2] give the highest performance, as they achieved the highest average accuracies of the five proposed classifiers. Accordingly, the three previously mentioned electrodes will be tried and analyzed in the following part as they are the most effective electrodes.

4.4. Fourth: Analyzing the performance of the three highest electrodes

As mentioned before: the highest three accuracies revealed from electrodes F4 (avg. acc. = 84.53%), O2 (avg. acc. = 83.18%), and CPZ (avg. acc. = 81.32%). Now, the accuracies of using those three electrodes separately against the accuracy of using them

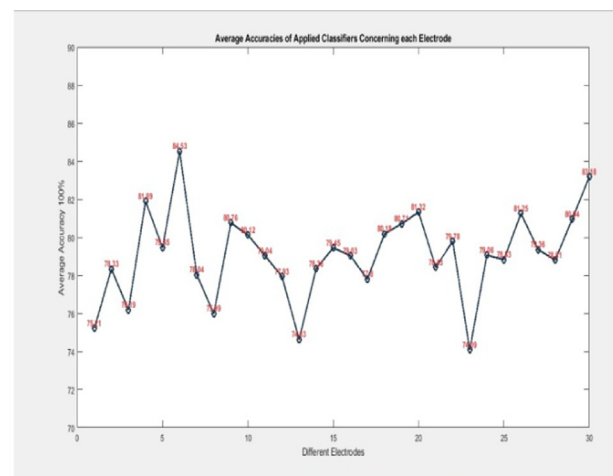
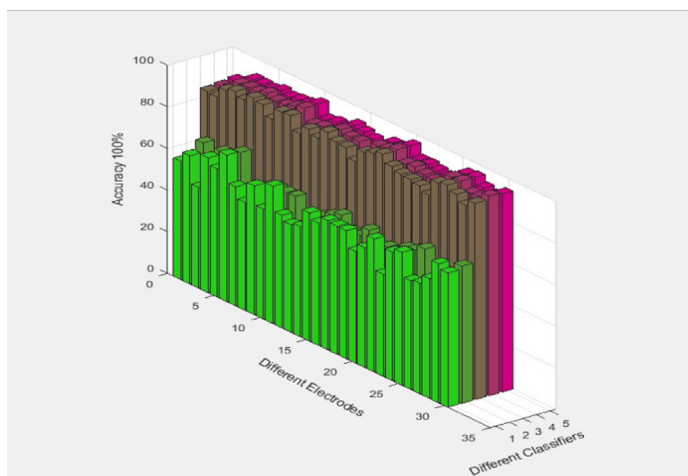


Fig. 10. Average accuracies of thirty electrodes.

simultaneously (concatenated) will be examined. The results are presented in Fig. 11.

From Fig. 11 it can be noticed that working on electrodes F4, CPZ, and O2 together (concatenated) yields very good results

which means that working on the reduced number of electrodes from thirty to only three is much better as the accuracies are very high and the processing time will be highly decreased making this tool more reliable, effective and robust.

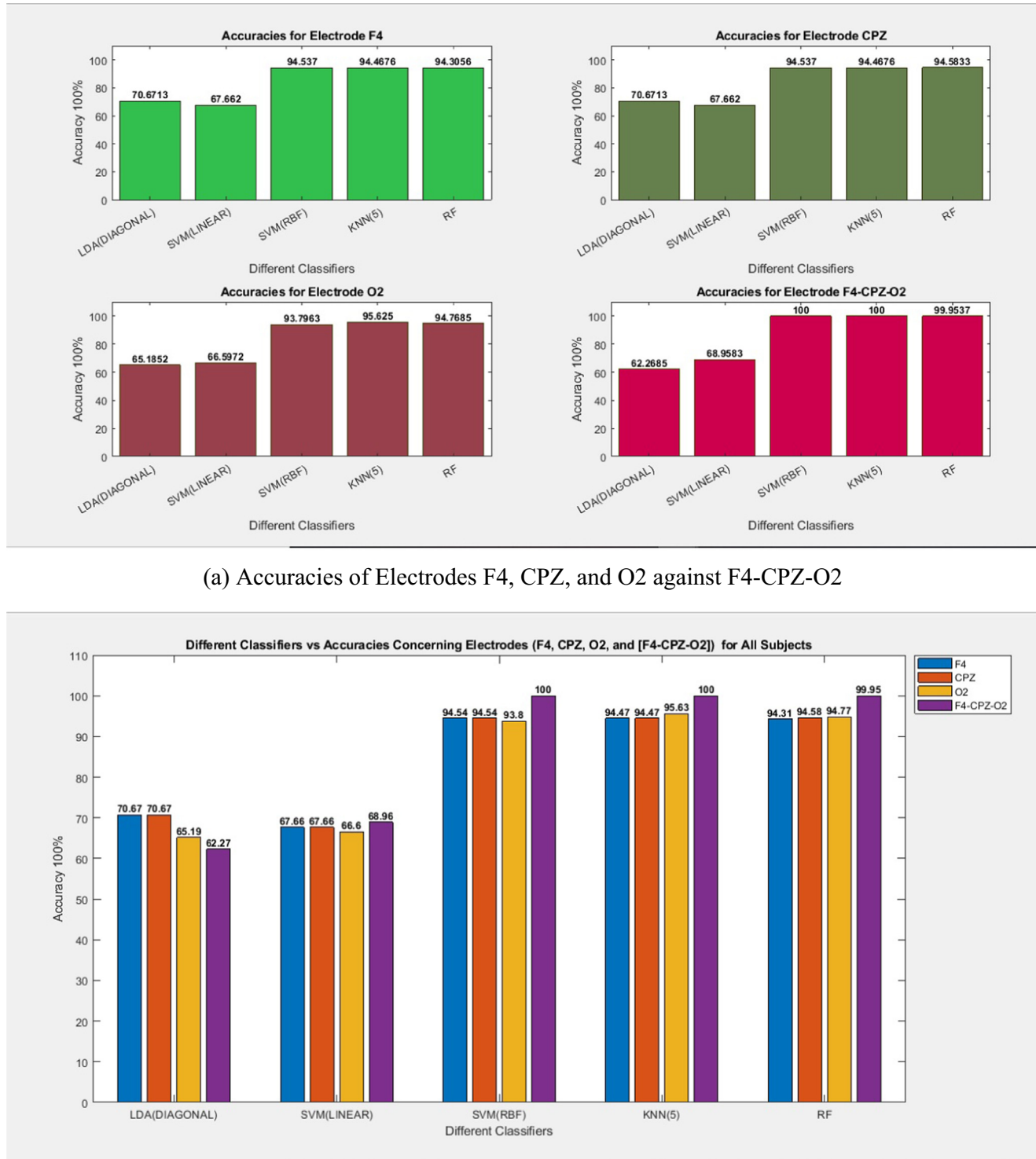


Fig. 11. Different Classifiers vs Accuracies Concerning Electrodes (F4, CPZ, O2, and [F4-CPZ-O2]) for All Subjects.

4.5. Fifth: Only three electrodes

From the previously presented work, the full details concerning the classifiers' performances and the confusion matrices dealing with the electrodes (F4-FCZ-O2) will be shown in the following part.

The four possible observations, where positive means target (Fatigue/Drowsy) and negative means non-target (Normal/Alert):

- Observation is positive and is predicted to be positive: True positives (T.P.).
- Observation is negative and is predicted to be negative: True negatives (T.N.).
- Observation is negative but is predicted positive: False positives (F.P.).
- Observation is positive but is predicted negative: False negatives (F.N.).

Therefore, four classifiers' performances and evaluation measurements will be computed: accuracy, sensitivity, specificity, and precision.

The actual and predicted testing data are 4320 observations (7200 observations [3600 N and 3600F] X 60% "The testing part").

The confusion matrices for the five presented classifiers are shown in Table 7 for all subjects.

Table 8 shows the accuracies calculations for the five classifiers performed on all participants' (subjects') data using only three electrodes (F4, FCZ, and O2).

The Receiver Operating Characteristic (ROC) Curve is a common visual representation of a classification model's output. It summarizes the trade-off between the true positive rate (TPR) and the

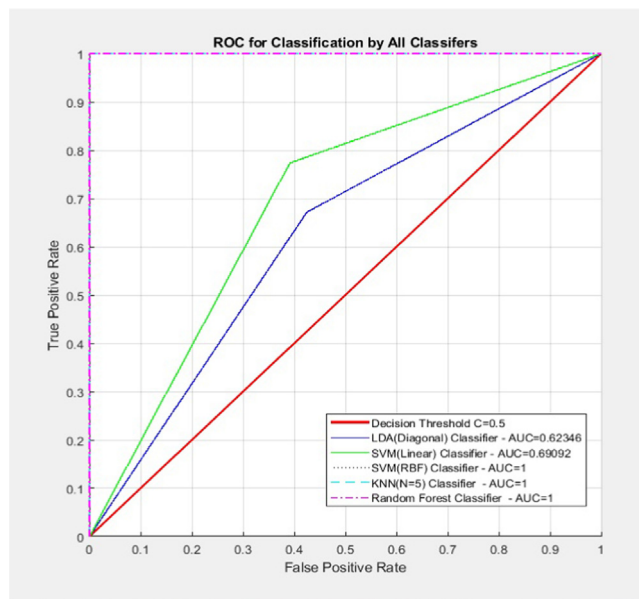


Fig. 12. ROC Curves of the Applied Classifiers.

Table 7

Confusion Matrices for All Applied Classifiers Regarding the Data of The Three Electrodes from All Subjects.

		Actual Value	
		(Target)Positive	(Non-Target)Negative
Predicted Value	(Target)Positive (Non-Target)Negative	T.P. = 1427 F.N. = 698	F.P. = 932 T.N. = 1263
LSVM		Actual Value	
		(Target)Positive	(Non-Target)Negative
Predicted Value	(Target)Positive (Non-Target)Negative	T.P. = 1644 F.N. = 481	F.P. = 860 T.N. = 1355
SVM (RBF)		Actual Value	
		(Target)Positive	(Non-Target)Negative
Predicted Value	(Target)Positive (Non-Target)Negative	T.P. = 2125 F.N. = 0	F.P. = 0 T.N. = 2195
KNN(N=5)		Actual Value	
		(Target)Positive	(Non-Target)Negative
Predicted Value	(Target)Positive (Non-Target)Negative	T.P. = 2125 F.N. = 0	F.P. = 0 T.N. = 2195
Random Forest(T = 10)		Actual Value	
		(Target)Positive	(Non-Target)Negative
Predicted Value	(Target)Positive (Non-Target)Negative	T.P. = 2122 F.N. = 3	F.P. = 0 T.N. = 2195

Table 8

Accuracies Calculations for All Applied Classifiers.

Classifiers	From electrodes (F4, FCZ, and O2) for all subjects			
	Accuracy	Precision	Sensitivity	Specificity
DiagLDA	62.2685%	60.4917%	67.1529%	63.6485%
SVM (Linear)	69.0923%	65.6549%	77.3647%	71.0304%
SVM (RBF)	100%	100%	100%	100%
KNN (N = 5)	100%	100%	100%	100%
Random Forest (T = 10)	99.931%	100%	99.8588%	99.9294%

Table 9

Accuracies from Various Researchers.

#	Research Group	Acc.	Center of Research	Differences
1	Jianliang Min [51]	98.3%	The Center of Collaboration and Innovation, Jiangxi University of Technology, Nanchang, China	Features: Multiple Entropy Fusion
2	Zhang [23]	96.5%	Northeastern University Shenyang, China	Features: Entropy and Complexity Measure
3	Nugraha [68]	96%	Department of Informatics, Institut Teknologi Sepuluh Nopember, Indonesia	Using Emotiv EPOC+
4	Yin J [69]	95%	The Center of Collaboration and Innovation, Jiangxi University of Technology, Nanchang, China	Using Fuzzy Entropy Method
5	Xiong [39]	90%	College of Mechanical and Electrical Engineering, Wuhan Donghu University, Wuhan 430212, China	Using Approximate Entropy and Sample Entropy
6	Ko [70]	90%	Brain Research Center and I-RiCE Center, National Chiao-Tung University, Hsinchu, Taiwan	Using Fast Fourier Transformation
7	Chai [71]	88.2%	Krida Wacana Christian University, Jakarta, Indonesia	Using Entropy Rate Bound Minimization Analysis
8	Mu Z [72]	85%	Institute of Information Technology, Jiangxi University of Technology, Nanchang, China	Using EEG Frequency Ratio
9	Correa [73]	83.6%	Gabinete de Tecnología Médica, Facultad de Ingeniería, Universidad Nacional de San Juan (UNSJ), San Juan, Argentina	Using Multimodal Analysis
10	Wang [74]	83%	School of Electrical Engineering and Automation, Harbin Institute of Technology, Harbin, China	Using Power Spectral Density
11	This work	100%	Misr University for Science and Technology, Faculty of Engineering, Giza, Egypt	Using EEG Waveform shape as a feature

false positive rate (FPR) for various likelihood thresholds in a predictive model. ROC curves for all subjects for the five classifiers presented in Fig. 12 clearly depicts EEG data obtained from (F4-FCZ-O2) electrodes.

Tables 8 and 9 show that all the accuracies calculations give high results for all suggested classifiers. In the ROC curves analysis shown in Fig. 12, it is obvious that the areas under the ROC curves (AUC) give high results (more than 0.99) of the applied classifiers (SVM[RBF], KNN[N = 5], and RF[T = 10]). This means that the proposed classifiers are appropriate models.

4.6. Comparative analysis

Several research groups have used EEG signals to study driver fatigue detection in recent years to resolve this issue. Table 9 describes the related classification methods used in some studies. This indicates that the results obtained by applying the proposed classification methods were better than that presented below in Table 9 despite utilizing fewer features extracted from only three electrodes,

In traffic safety, detecting driver exhaustion has a clear application for warning of driving fatigue and minimizing unnecessary driving accidents. Future research should concentrate on two areas:

1. The variability of fatigue data along time.
2. The practical presentation of an EEG-based fatigue navigation system.

The time variability of fatigue data can aid in determining the degree of uncertainty in a system's data variables and capturing the sensitivity of the obtained results [75,76]. EEG datasets from another online experiment in this study were subjected to an off-line review. Since the offline and online classifications have different features, a follow-up analysis in a real-time online experimental setting is required to validate the results of this study [66].

5. Conclusion

An objective method for detecting drowsy driving in an EEG-based framework was suggested in this study. Five classifiers were utilized for training and testing data: Diagonal Linear Discriminant

Analysis (DiagLDA), Support Vector Machine (Linear and Radial Basis Functions), K-Nearest Neighbor (KNN), and Random Forest Classifier (RF). Data were preprocessed before extracting features, and an easily electrode chosen technique was utilized to optimize electrodes and demonstrate the efficacy and robustness of the proposed method. It reported high performance with just three electrodes as the accuracy reached 100% for LSVM and KNN classifiers. The results suggested that this type of technology could be useful for detecting drowsy driving.

It is predicted that an EEG-based system for drowsiness observation in appropriate areas, or a competitive function with presented methods, would be feasible. Although, there are many problems in the future that will need to be addressed. The study needs to be replicated with a large group of people and real-world driving EEG accuracies. The reliability and comfort of different frequency bands using other features for real-time monitoring of driver drowsiness should be the subject of future studies.

Declaration of Competing Interest

The authors declare that they have no known competing financial interests or personal relationships that could have appeared to influence the work reported in this paper.

Acknowledgment

The author would like to thank the providers of the EEG Dataset (Jianliang Min, Jianliang Min, Ping Wang, Ping Wang, and Jianfeng Hu 2017).

Funding

No funding was received for conducting this study.

Data availability

The datasets analyzed during the current study are available in the repository: <https://doi.org/10.6084/m9.figshare.5202739.v1>. These datasets were derived from the following public domain resource:

https://figshare.com/articles/dataset/The_original_EEG_data_for_driver_fatigue_detection/5202739.

References

- [1] The European Commission, Directorate-General Transport and Energy- "Fatigue European Road Safety Observatory Report". www.erso.eu; 2006.
- [2] Anund A, Kircher K. Advantages and disadvantages of different methods to evaluate sleepiness warning systems. VTI Report, Sweden; 2009. Available from: www.vti.se/publications.
- [3] Larue GS, Rakotonirainy A, Pettitt AN. Predicting driver's hypo vigilance on monotonous roads literature review. In: 1st international conference on driver distraction and inattention, Gothenburg, Sweden, September 28–29; 2009.
- [4] Sahayadhas A, Sundaraj K, Murugappan M. Detecting driver drowsiness based on sensors: a review. *Sensors* 2012;12(12):16937–53.
- [5] Yu X. Integrated approach for nonintrusive detection of driver drowsiness. ITA Institute Report, Intelligent Transportation Systems Institute Center for Transportation Stud. Univ. of Minnesota; 2012.
- [6] Fuletra JD, Bosamiya D. A survey on driver's drowsiness detection techniques. *IJRITCC* 2013;1(11):816–9.
- [7] Brown T, Lee J, Schwarz C, Fiorentino D, McDonald A, Traube E, et al. Detection of driver impairment from drowsiness. In: 23rd international technical conference on the enhanced safety of vehicles, Seoul, South Korea; 2013.
- [8] Kang HB. Various approaches for driver and driving behavior monitoring: a review. In: Computer Vision Workshops (ICCVW), IEEE international conference; 2013. p. 616–23.
- [9] Hallvиг D, Anund A, Fors C, Kecklund G, Karlsson JG, Wahde M, et al. Sleepy driving on the real road and in the simulator - a comparison. *Accident Anal Prevention* 2013;50:44–50.
- [10] Jagannath M, Balasubramanian V. Assessment of early onset of driver fatigue using multimodal fatigue measures in a static simulator. *Appl Ergon* 2014;45(4):1140–7.
- [11] Chi YM, Ng P, Kang E, Kang J, Fang J, Cauwenberghs G. Wireless non-contact cardiac and neural monitoring. *Proc Wireless Health* 2010;15–23:2010.
- [12] Jana GC, Swetapadma A, Pattnaik PK. Enhancing the performance of motor imagery classification to design a robust brain computer interface using feed forward back-propagation neural network. *Ain Shams Eng J* 2018;9(4):2871–8.
- [13] rawat S, K. Verma V. A review on sleep detection using EEG signal. *IJETT* 2015;23(6):293–7.
- [14] Awais M, Badruddin N, Drieberg M. A simulator based study to evaluate driver drowsiness using electroencephalogram. intelligent and advanced systems (ICIAS). In: 5th international conference; 2014.
- [15] Brown T, Johnson R, Milavetz G. Identifying periods of drowsy driving using EEG. In: Annals of advances in automotive medicine conference, vol. 57; 2013.
- [16] Tran Y, Thuraisingham R, Wijesuriya N, Craig A, Nguyen H. Using S-transform in EEG analysis for measuring an alert versus mental fatigue state. Engineering in Medicine and Biology Society (EMBC). In: 36th annual international conference of the IEEE; 2014.
- [17] Li G, Chung W-Y. Estimation of eye closure degree using EEG sensors and its application in driver drowsiness detection. *Sensors* 2014;14(9):17491–515.
- [18] Li G, Chung W-Y. A context-aware EEG headset system for early detection of driver drowsiness. *Sensors* 2015;15(8):20873–93.
- [19] Li G, Lee B-L, Chung W-Y. Smart watch-based wearable EEG system for driver drowsiness detection. *Sensors* 2015;15(12):7169–80.
- [20] Golz M, Sommer D. Short-term EEG patterns of driver drowsiness and their relation to crashes. *Biomed Eng* 2015. doi: 10.1515/bmt-2013-4166.
- [21] Golz M, Sommer D, Trutsche U, Krajewski J, Sirois B. Driver drowsiness immediately before crashes – a comparative investigation of EEG pattern recognition. In: 7th international driving symposium on human factors in driver assessment, training, and vehicle design, New York; 2013.
- [22] Maglione, Borghini G, Aricò P, Borgia F, Graziani I, Colosimo A, et al. Evaluation of the workload and drowsiness during car driving by using high resolution EEG activity and neurophysiologic indices. Proceedings of the IEEE international conference. Engineering in Medicine and Biology Society, Chicago, IL, USA; 2014;26(30):6238–41.
- [23] Zhang C, Wang H, Fu R. Automated detection of driver fatigue based on entropy and complexity measures. *IEEE Trans Intelligent Transp Syst* 2014;15(1):168–77.
- [24] Wierwille WW, Ellsworth LA. Evaluation of driver drowsiness by trained raters. *Accid Anal Prev* 1994;26(5):571–81.
- [25] Wiegand DM, McClafferty J, McDonald SE, Hanowski RJ. Development and evaluation of a naturalistic observer rating of drowsiness protocol. NSTSC-E. Report, National Surface Transportation Safety Center for Excellence; 2009.
- [26] Anund A, Fors C, Hallvíg D, Åkerstedt T, Kecklund G, Timmer A. Observer rated sleepiness and real road driving: an explorative study. *PLoS ONE* 2013;8(5):e64782. doi: <https://doi.org/10.1371/journal.pone.0064782>.
- [27] Ahlstrom C, Fors C, Anund A, Hallvíg D. Video-based observer rated sleepiness versus self-reported subjective sleepiness in real road driving. *Eur Transp Res* Springer 2015;7(4). doi: <https://doi.org/10.1007/s12544-015-0188-v>.
- [28] Zhao C, Zheng C, Zhao M, Liu J, Tu Y. Automatic classification of driving mental fatigue with EEG by wavelet packet energy and KPCASVM. *ICIC* 2011;7(3):1157–68.
- [29] Zhao C, Zheng C, Zhao M, Liu J. Physiological assessment of driving mental fatigue using wavelet packet energy and random forests. *Am J Biomed Sci* 2010;262–74.
- [30] Abdel-Rahman AS, Seddik AF, Shawky DM. Development of a wireless safety helmet mobile APP using EEG signal analysis development of a wireless safety helmet mobile APP using EEG signal analysis. *Int J Signal Processing Syst IJSPS* 2016;432–6. doi: <https://doi.org/10.18178/ijspcs.4.5.432-436>.
- [31] Abdelrahman AS, Seddik AF, Shawky DM. A low-cost drowsiness detection system as a medical mobile application. In: 37th Annual international conference of the IEEE Engineering in Medicine and Biology Society, EMBC'15; 2015.
- [32] Lee B-G, Lee B-L, Chung W-Y. mobile healthcare for automatic driving sleep-onset detection using wavelet-based EEG and respiration signals. *Sensors* 2014;14(10):17915–36.
- [33] Li W, He Q-C, Fan X-M, Fei Z-M. Evaluation of driver fatigue on two channels of EEG data. *Neurosci Lett* 2012;506(2):235–9.
- [34] Chai R, Tran Y, Craig A, Ling S, Nguyen H. Enhancing accuracy of mental fatigue classification using advanced computational intelligence in an electroencephalography system. In: Proc. the 36th annual int. conf. of the IEEE Engineering in Medicine and Biology Society (EMBC); 2014. p. 1338–41.
- [35] Tsai PY, Hu W, Kuo TBJ, Shyu L-Y. A portable device for real-time drowsiness detection using novel active dry electrode system. In: 31st annual international conference of the IEEE; 2009.
- [36] Murugappan M, Wali MK, Ahmmd RB, Murugappan S. Subtractive fuzzy classifier based driver drowsiness levels classification using EEG. In: International conference on communication and signal processing, IEEE; 2013.
- [37] Wali MK, Murugappan M, Ahmmd RB. PNN based driver drowsiness level classification using EEG. *JATIT* 2013;52(3).
- [38] San PP, Ling S, Chai R, Tran Y, Craig A, Nguyen H. EEG-based driver fatigue detection using hybrid deep generic model. In: Proceedings of the 38th annual international conference of the IEEE Engineering in Medicine and Biology Society 2016. p. 800–3.
- [39] Xiong Y, Gao J, Yang Y, Yu X, Huang W. Classifying driving fatigue based on combined entropy measure using EEG signals. *Int J Control Automation* 2016;9(3):329–38.
- [40] Mardi Z, Ashtiani SN, Mikaili M. EEG-based drowsiness detection for safe driving using chaotic features and statistical tests. *J Med Signals Sensors* 2011;1(2):130. doi: <https://doi.org/10.4103/2228-7477.95297>.
- [41] Goovaerts G, Denissen A, Milošević M, Boxtel G, Huffel S. Advanced EEG processing for the detection of drowsiness in drivers. In: Proc. Int. BIOSIGNALS Conf., March 2014. p. 205–212.
- [42] Eoh HJ, Chung MK, Kim S-H. Electroencephalographic study of drowsiness in simulated driving with sleep deprivation. *Int J Ind Ergon* 2005;35(4):307–20.
- [43] Jap B, Lal S, Fischer P. Inter-hemispheric electroencephalography coherence analysis: assessing brain activity during monotonous driving. *Int J Psychophysiol* 2010;169–73.
- [44] Rost M, Zilberg E, Xu1 Z, Feng Y, Burton D, Lal S. Comparing contribution of algorithm based physiological indicators for characterization of driver drowsiness. *J Med. Bioeng.* 2015;4(5).
- [45] Li P, Jiang W, Su F. Single-channel EEG-based mental fatigue detection based on deep belief network. In: 38th annual international conference of the IEEE Engineering in Medicine and Biology Society (EMBC) 2016. p. 367–70.
- [46] Kar S, Bhagat M, Routray A. EEG signal analysis for the assessment and quantification of driver's fatigue. *Transp Res* 2010;13(5):297–306.
- [47] Balam VP, Sameer VU, Chinara S. Automated classification system for drowsiness detection using convolutional neural network and electroencephalogram. *IET Intell Transp Syst* 2021;15:514–24.
- [48] Chaabene S, Bouaziz B, Boudaya A, Hökelmann A, Ammar A, Chaari L. Convolutional neural network for drowsiness detection using EEG signals. *Sensors* 2021;21(5):1734. doi: <https://doi.org/10.3390/s21051734>.
- [49] Jiao Y, Deng Y, Luo Y, Lu B-L. Driver sleepiness detection from EEG and EOG signals using GAN and LSTM networks. *Neurocomputing* 2020;408:100–11.
- [50] Zou S, Qin T, Huang P, Bai X, Liu C. Constructing multi-scale entropy based on the empirical mode decomposition (EMD) and its application in recognizing driving fatigue. *J Neurosci Methods* 2020;341:108691.
- [51] Min J, Wang P, Hu J, Lei Xu. Driver fatigue detection through multiple entropy fusion analysis in an EEG-based system. *PLoS ONE* 2017;12(12):e0188756. doi: <https://doi.org/10.1371/journal.pone.0188756>.
- [52] Min Jianliang, Wang Ping, Hu Jianfeng. The original EEG data for driver fatigue detection 2017. Figshare Dataset. doi: 10.6084/m9.figshare.5202739.v1.
- [53] Duda RO, Hart PE, Stork DG. Pattern recognition. 2nd ed. WILEY-INTERSCIENCE; 2001.
- [54] Fukunaga K. Statistical pattern recognition. 2nd edition. ACADEMICPRESS, INC; 1990.
- [55] Burges CJC. A tutorial on support vector machines for pattern recognition: knowledge discovery and data mining. 1998;2:121.
- [56] Bennett KP, Campbell C. Support vector machines: type explorations Newsletter, 2000; 2:1.
- [57] Blankertz B, Kawanabe M, Tomioka R, Hohlfeld F, Müller K-R, Nikulin VV. Invariant common spatial patterns: ALLEVIATING nonstationarities in brain-computer interfacing. *Adv Neural Inf Process Syst* 2007;113–20.
- [58] Garrett D, Peterson DA, Anderson CW, Thaut MH. Comparison of linear, nonlinear, and feature selection methods for EEG signal classification. *IEEE Trans Neural Syst Rehabil Eng* 2003;11(2):141–4.
- [59] Rakotomamonjy A, Guigue V, Mallet G, Alvarado V. Ensemble of SVMs for improving brain computer interface P300 speller performances. In: International conference on artificial neural networks; 2005.
- [60] Rakotomamonjy A, Guigue V. BCI competition III: Dataset II - ensemble of SVMs for BCI P300 speller. *IEEE Trans Biomed Eng* 2008;55:1147.

- [61] Jain AK, Duin PW, Jianchang Mao. Statistical pattern recognition: a review. *IEEE Trans Pattern Anal Mach Intell* 2000;22(1):4–37.
- [62] Hastie T, Tibshirani R, Friedman J. *The elements of statistical learning: data mining, inference and prediction*. Springer; 2009.
- [63] Manning CD, Raghavan P, Schütze H. *Introduction to Information Retrieval*. Cambridge University; 2008.
- [64] Olson M. Essays on random forest ensembles. Ph.D. Thesis. 3420 Walnut St., Philadelphia, PA 19104-6206; 2018.
- [65] Hsu Chih-Wei, Chih-Chung Chang, Chih-Jen Lin. A Practical Guide to Support Vector Classification. National Taiwan University, May 2016. Available from: <https://www.csie.ntu.edu.tw/~cjlin/papers/guide/guide.pdf>.
- [66] Fouad IA, Labib F-Z, Mabrouk MS, Sharawy AA, Sayed AY. Improving the performance of P300 BCI system using different methods. *Netw Model Anal Health Inform Bioinforma* 2020;9(1). doi: <https://doi.org/10.1007/s13721-020-00268-1>.
- [67] Labib F-Z, Fouad IA, Mabrouk MS, Sharawy AA. Multiple classification techniques toward a robust and reliable P300 BCI system. *Biomed Eng Appl Basis Commun* 2020;32(02):2050010. doi: <https://doi.org/10.4015/S1016237220500106>.
- [68] Nugraha BT, Sarno R, Asfani DA, Igasaki T, Munawar MN. Classification of driver fatigue state based on EEG using Emotiv EPOC+. *J Theor Appl Inf Technol* 2016;86(3):347±59.
- [69] Yin J, Hu J, Mu Z. Developing and evaluating a mobile driver fatigue detection network based on electroencephalograph signals. *Healthcare Technol Lett* 2017;4(1):34–8.
- [70] Ko LW, Lai WK, Liang WG, Chuang CH, Lu SW, Lu YC, et al. Single channel wireless EEG device for real-time fatigue level detection. In: International joint conference on neural networks; 2015. p. 1–5.
- [71] Chai R, Naik GR, Nguyen TN, Ling SH, Tran Y, Craig A, et al. Driver fatigue classification with independent component by entropy rate bound minimization analysis in an EEG-based system. *IEEE J Biomed Health Informatics* 2017;21(3):715–24.
- [72] Mu Z, Yin J, Hu J. Mobile healthcare system for driver based on drowsy detection using EEG signal analysis. *Metall Mining Industry* 2015;7(7):266±73.
- [73] Garcés Correa A, Orosco L, Laciár E. Automatic detection of drowsiness in EEG records based on multimodal analysis. *Med Eng Phys* 2014;36(2):244–9.
- [74] Wang Y, Liu X, Zhang Y, Zhu Z, Liu D, Sun J. Driving fatigue detection based on EEG signal. In: Fifth international conference on instrumentation and measurement, computer, communication and control; 2015. p. 715±9.
- [75] Convertino M, Muñoz-Carpena R, Kiker GA, Perz SG. Design of optimal ecosystem monitoring networks: hotspot detection and biodiversity patterns. *Stoch Env Res Risk Assess* 2015;29(4):1085–101.
- [76] Lüdtke N, Panzeri S, Brown M, Broomhead DS, Knowles J, Montemurro MA, et al. Information-theoretic sensitivity analysis: a general method for credit assignment in complex networks. *J R Soc Interface* 2008;5(19):223–35.



Islam A. Fouad is an Assistant Professor at the Department of Biomedical Engineering-Faculty of Engineering at Misr University for Science and Technology, 6th October, Egypt. He received his PhD in System and Biomedical Engineering in 2014 from Cairo University, Egypt. His research interests are in the areas of digital image processing, microarray image analysis, brain computer interface and computer-aided diagnosis. He has several research papers published in peer-reviewed international journals. Dr. Islam serves also as a reviewer for different highly reputation journals in related fields.